CHAPTER IV

RESULTS AND DISCUSSION

The characteristics of *A. incisus* extract

The appearance, moisture content and percent yield of the extract obtained from diethyl ether extraction are shown in Table 1 and Figure 16.

Table 1 The appearance, percentage of yield and moisture content of the *A. incisus*'s heartwood extract

Characteristics	*A. incisus*'s heartwood extract
% yield [a)]	0.94
% moisture content [b)]	6.98±0.56
Appearance	yellow powder

1. The percent yield of the *A. incisus* extract was calculated the weight by using the following equation:

% yield = [dry extract wt (g) / plant material sample wt (g)] x 100

2. The moisture content of the *A. incisus* extract was measured by using SARTORIOUS, model MA30 and then was calculated with the following equation:

% moisture content = [(initial wt (g) – final wt (g))/ initial wt (g)] x 100

The conditions and the content of moisture are shown in Table 2:

Table 2 The conditions and moisture content of *A. incisus*'s heartwood extract

Samples	Temperature (°C)	Time (min)	% Moisture content
A. incisus ether extract	105	6.2	6.98±0.56

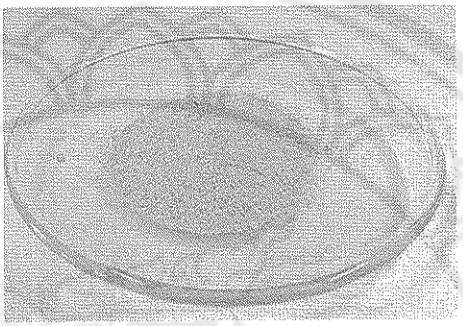

Figure 16 The appearance of *A. incisus* diethyl ether extract.

The appearance of *A. incisus* diethyl ether extract was yellow powder, as shown in Figure 16, which would be comfortable for storage. This result corresponds with the previous study that indicated diethyl ether extract provided yellow powder solid whereas that of the methanol provided deep brown paste [3]. The diethyl ether extract of *A. incisus*'s heartwood would be used for further studies to simplify its action on the melanogenesis inhibitory, antioxidant and anti-inflammatory activities.

The content of artocarpin in *A. incisus* extract

The HPLC chromatograms of the artocarpin standard and the samples are shown in Figure 17-19. The content of artocarpin in each sample was calculated from the calibration curve equation, as shown in Figure 20.

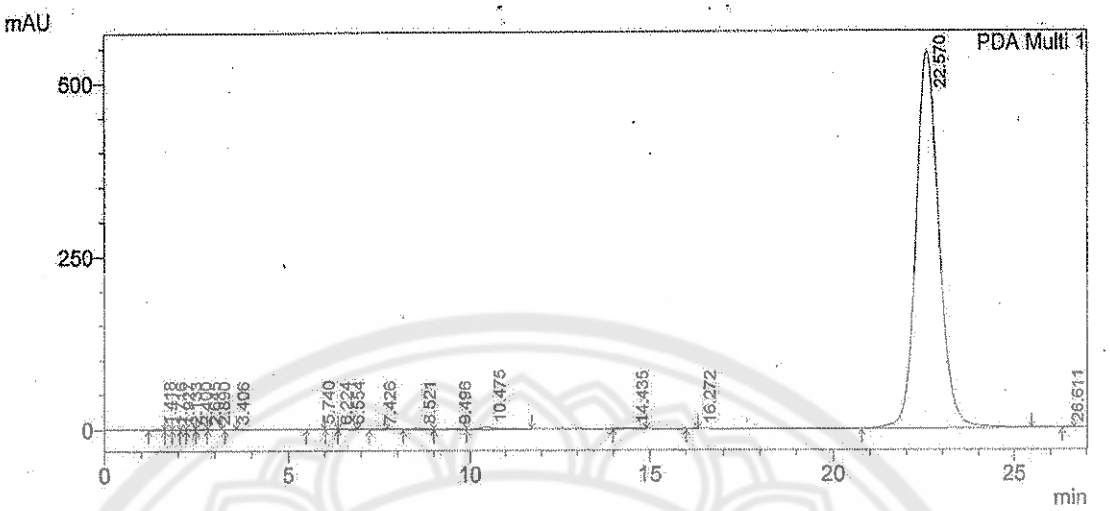

Figure 17 Chromatogram of 0.2 mg/ml artocarpin standard.

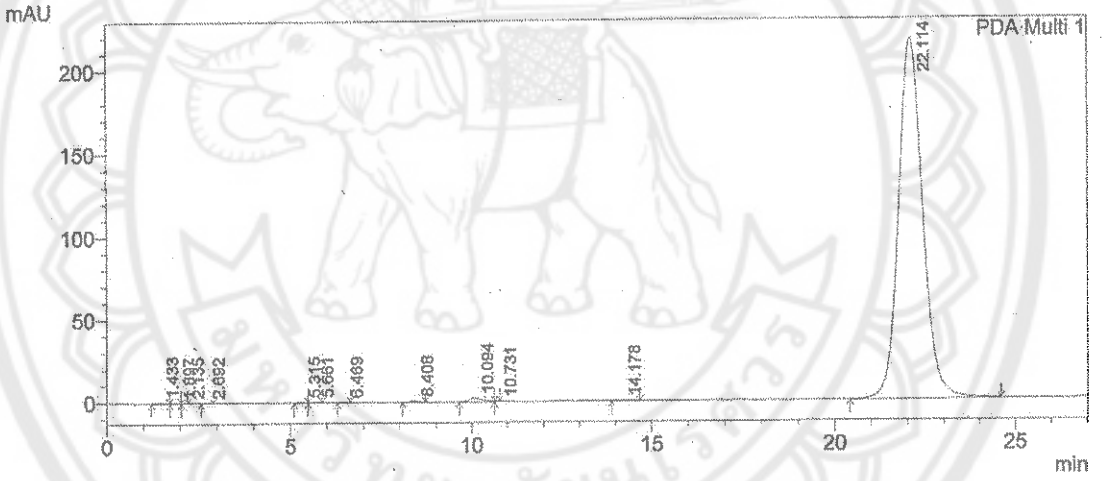

Figure 18 Chromatogram of 0.04 mg/ml artocarpin standard.

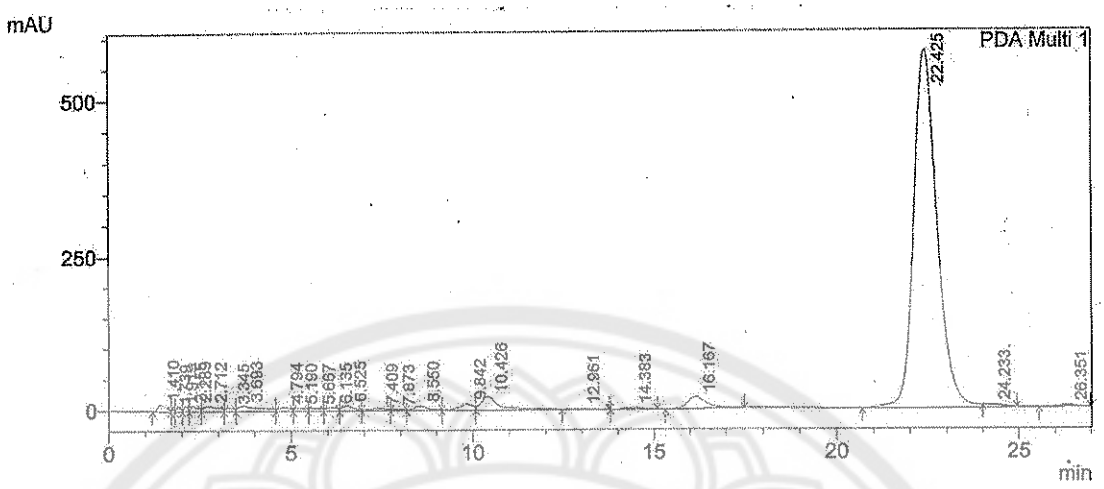

Figure 19 Chromatogram of 1.0 mg/ml *A. incisus* ether extract.

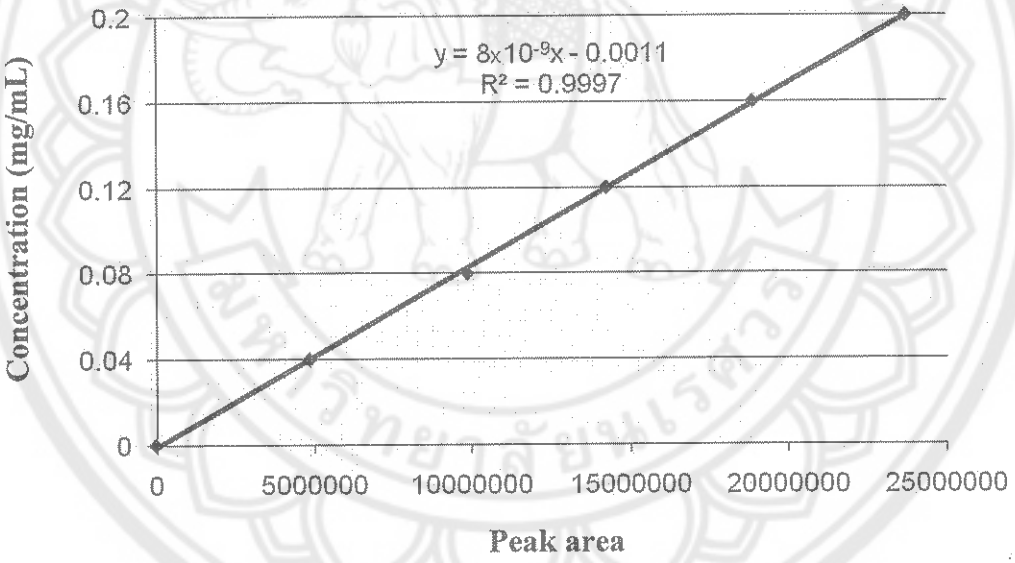

Figure 20 The calibration curve of artocarpin satandard.

From the HPLC experiment, this condition gave a well resolved and sharp peak for artocarpin with a retention time of approximately 22 min with no interference as shown in Figure 17-19. The amount of artocarpin in the ether extract was 44.4±0.1% w/w (Appendix A). This result corresponds with the previous study which artocarpin contained in the ether extract was 45.2±0.5% w/w [3].

***In vitro* efficacy of *A. incisus* extract on melanogenesis inhibition**

1. The study of B16F1 growth curve

Generally, this cell line shows a fast growth with a population doubling time that was dependent on seeding density [3]. A growth curve of the mouse melanoma cell line cultured in one condition is shown in Figure 21. The results showed that cells exhibited exponential growth up to 4 days, and discontinued to grow after 5 days of cultivation under the studied conditions. In addition, the observation under a microscope revealed that cells were confluent at day 5. Consequently, an incubation period of 4 days (within the log phase) was chosen to examine the effects of *A. incisus* extract on the melanin production.

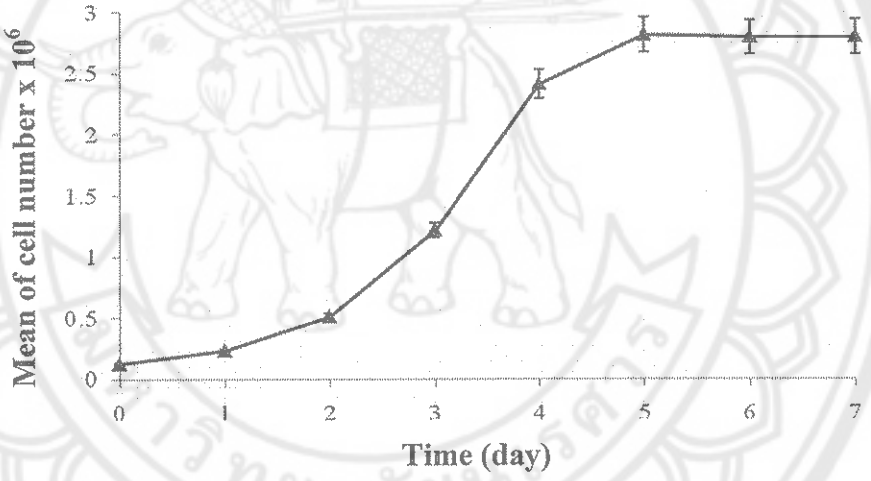

Figure 21 Growth curve of melanocyte B16F1 mouse melanoma cell line (Each point represents mean±S.D. of triplicate study).

The morphology of B16F1 mouse melanoma cells was dendritic cell. After seeding, attaching and spreading the melanocytes were clearly visible within 24 hr and confluent growth was observed at day 5 as shown in Figure 22.

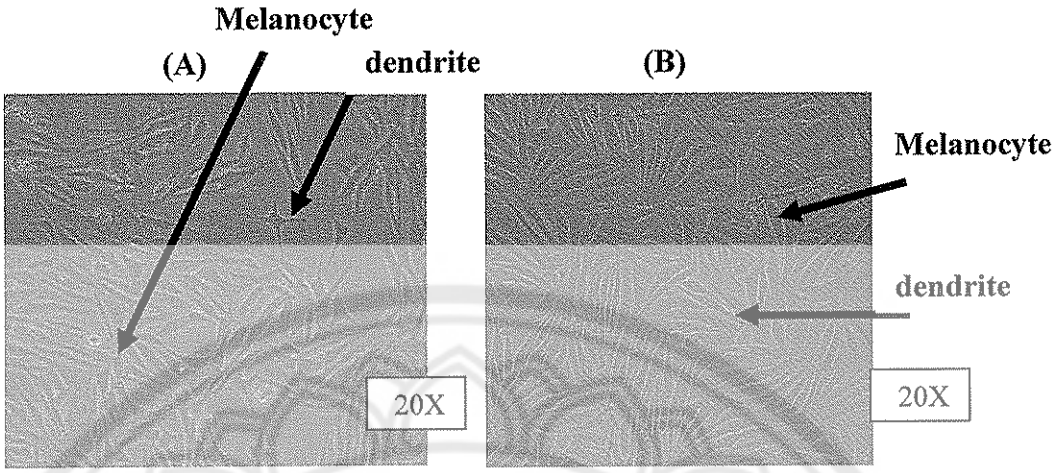

Figure 22 Morphology of melanocyte B16F1 melanoma cells of day 1 (A) and day 5 (B) at magnification of 20X.

2. Effect of *A. incisus* ether extract on melanin production

The efficiency on melanin production was determined by measuring the melanin content in cells after being treated with *A. incisus* extract or kojic acid. The *A. incisus* extract exhibited a dose-dependent inhibition of melanin production in B16F1 cells, as shown in Figure 23. The percentages of melanin reduction compared to the control at the concentrations of 10, 15, 25, 40, 80 and 100 µg/mL of *A. incisus* extract were 10.2±2.9%, 18.4±1.6%, 26.6±3.0%, 49.7±2.1%, 56.3±3.3% and 59.6±2.5%, respectively (Appendix B).

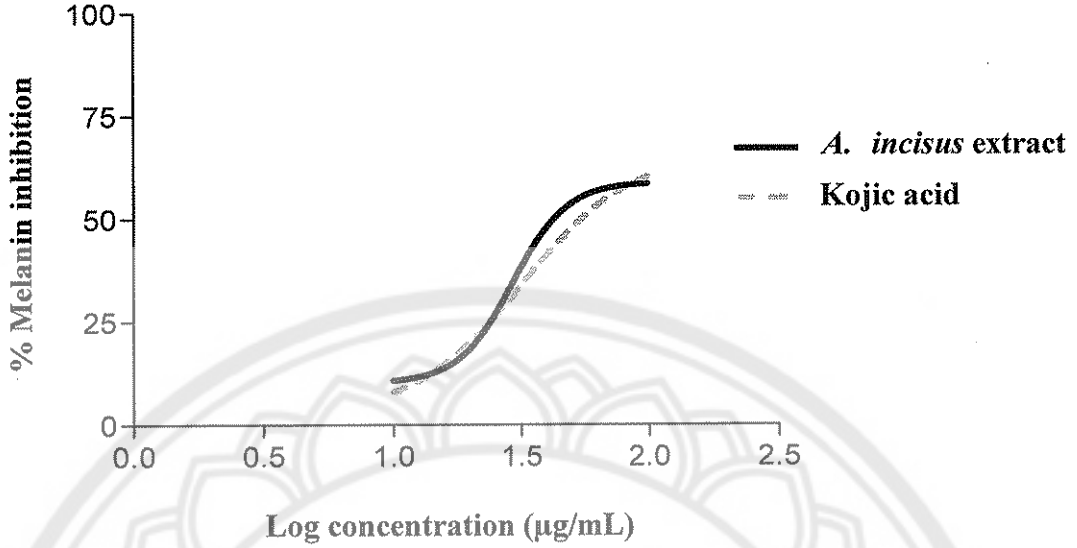

Figure 23 Inhibitory effects of *A. incisus* extract and kojic acid on melanin Synthesis in B16F1 cells (Data are expressed as percent of control, and each point represents mean±S.D. of triplicate study).

The results indicated that *A. incisus* extract showed higher inhibitory activity on melanogenesis than kojic acid in the cell culture. The IC_{50} for melanogenesis inhibition was 43.5±2.3 µg/mL whereas kojic acid exhibited melanogenesis inhibition activity with the IC_{50} of 57.6±1.3 µg/mL, as shown in Figure 23. There have been reported that kojic acid showed low- or non-inhibitory activity on the production of melanin in Melan-a [87, 88]. Because of its stability, kojic acid has limited use especially as a solution [89]. The lipophilic system of cell membrane may decrease the penetration of kojic acid through the cell, resulting in lower inhibitory action on intracellular tyrosinase enzyme [3]. Additionally, the effect of 40 µg/mL of kojic acid and 40 µg/mL *A. incisus* ether extract on proliferation and morphology of melanocyte cells are shown in Figure 24 and 25. The results under the microscopic observation revealed that kojic acid at the concentration of 40 µg/mL changed morphology of the melanocytes by losing dendrites (Figure 24) whereas *A. incisus* extract at the same concentration had no effect on the cell morphology as shown in Figure 25. It is possible that the extract contains some components which are contributing cell

structure by stabilization and/or protecting cell from damage in response to external stimuli [3].

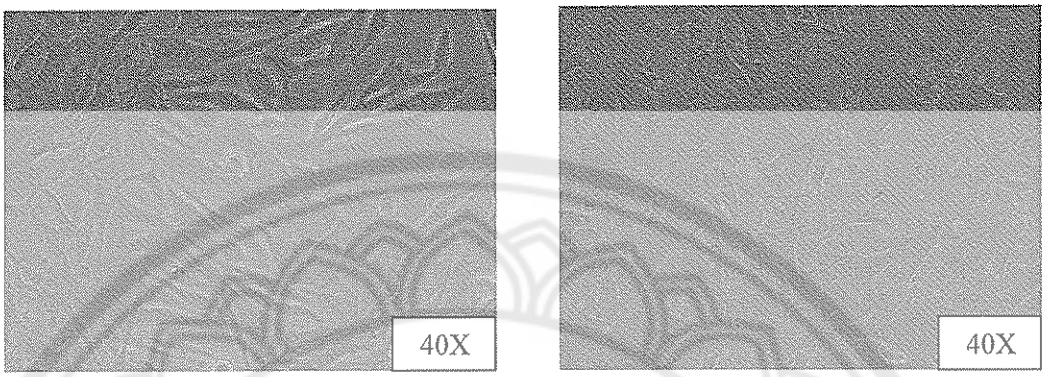

Figure 24 Morphology of melanocyte B16F1 melanoma cells after being treated with 0.1% DMSO (control) and with 40 μg/mL Kojic Acid for 4 days at magnification of 40X.

Figure 25 Morphology of melanocytes B16F1 melanoma cells after being treated with 0.1% DMSO (control) and with 40 μg/mL of *A. incisus* extract for 4 days at magnification of 40X.

3. Effect of *A. incisus* extract on cell proliferation

The number of viable cells after treated with various concentrations (10, 40 and 100 μg/mL) of *A. incisus* ether extract were evaluated by staining the cells with trypan blue dye to examine the effect of the ether extract on melanocyte B16F1 mouse melanoma cell proliferation. A dose-dependent inhibition on cell proliferation of *A. incisus* extract is shown in Figure 26. The significant inhibitory effect on B16F1 cell growth was observed at the concentration of 100 μg/mL compared with that of a low dose (< 40 μg/mL) of the extract. The result indicated that high dose of the extract may effect to alteration of cell attachment which is an influential characteristic for proliferation of cell.

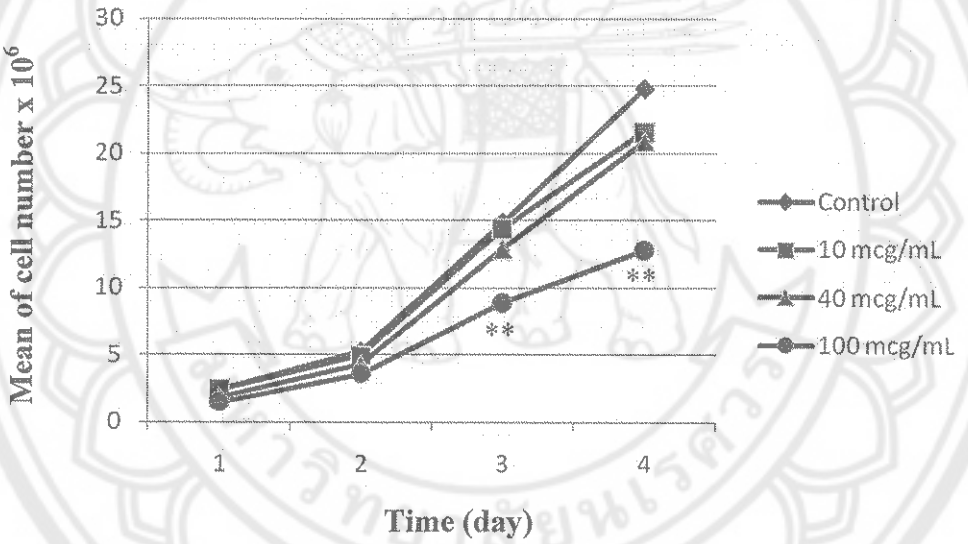

Figure 26 The effect of *A. incisus* on melanocyte B16F1 melanoma cells number (Each point represents mean±S.D. of triplicate study. Significant differences from control; **p<0.01).

***In vitro* antioxidant activity of *A. incisus* extract**

In the present study *A. incisus* extract was evaluated for its ability to neutralize the stable free radicals such as DPPH radicals. The EC_{50} values of *A. incisus* extract and the positive controls are presented in Table 3 to 5 (Appendix C).

Table 3 The percentage of free radical scavenging of *A. incisus* extract dissolved in DMSO.

Concentration of *A. incisus* extract / DMSO (µg/mL)	Free radical scavenging (%)	EC_{50} (µg/mL)
0.5	3.5±0.2	168.6±6.8
1	7.5±0.3	
5	10.2±0.4	
10	12.9±0.6	
50	19.8±0.2	
100	41.3±1.1	
250	62.8±1.6	
500	76.7±1.6	
1000	85.0±1.4	
2000	93.9±0.2	

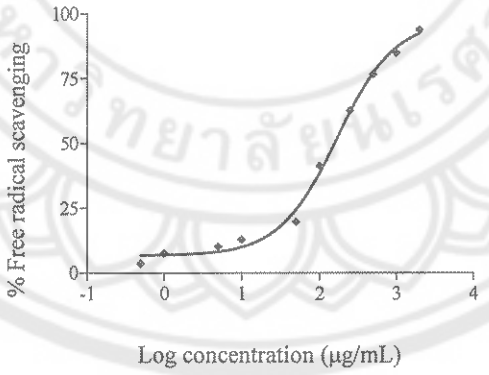

Figure 27 Antioxidant activity of *A. incisus* extract.

Table 4 The percentage of free radical scavenging of L-ascorbic acid dissolved in deionized water.

Concentration of L-ascorbic acid / water (μg/mL)	Free radical scavenging (%)	EC_{50} (μg/mL)
0.25	8.6±05	5.0±0.1
0.5	14.7±0.3	
2.5	42.5±1.5	
5	68.7±0.2	
25	87.0±0.4	
50	95.8±0.2	
125	94.8±0.3	
250	95.0±0.3	
1000	95.4±0.2	
2500	95.5±0.2	

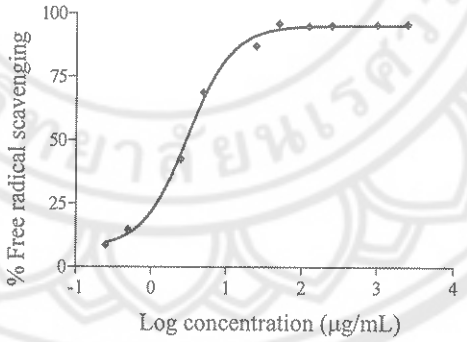

Figure 28 Antioxidant activity of L-ascorbic acid.

Table 5 The percentage of free radical scavenging of butylated hydroxytoluene (BHT) dissolved in methanol

Concentration of BHT / methanol (μg/mL)	Free radical scavenging (%)	EC_{50} (μg/mL)
0.25	13.5±0.5	3.2±0.2
0.5	15.9±0.6	
2.5	55.7±0.4	
5	81.0±0.2	
25	93.1±0.7	
50	94.6±0.6	
125	95.5±0.8	
250	96.8±0.2	
1000	97.1±0.5	
2500	96.7±0.4	

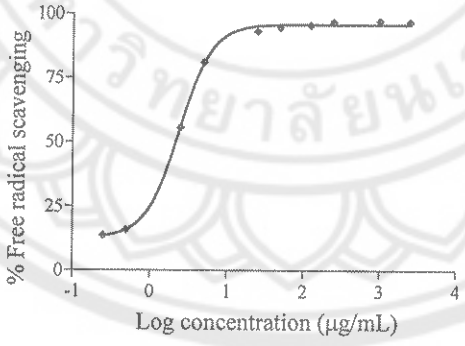

Figure 29 Antioxidant activity of *A. incisus* ether extract, L-ascorbic acid and butylated hydroxytolue (BHT).

The results indicated that the *A. incisus* extract showed less scavenging activity than BHT and L-ascorbic acid. Therefore, the *A. incisus* extract may exhibit weak scavenging activity. However, the results gained from this assay provided simple data that tested only recognizes free radical scavenging effects and not pro-oxidant activity [48]. Additionally, most compounds showed significant differences in free radical scavenging activity according to the method used [87]. In general, many plant phenolics have antioxidant activity [88], and various naturally occurring anti-melanogenic reagents contain a phenolic structure such as *Pharbitis nil*, *Sophora japonica*, *Spatholobus suberectus*, and *Morus alba* [89-91]. Its antioxidant property may prevent or delay pigmentation by different mechanism, such as by scavenging ROS and reactive nitrogen species [92], or by reducing *o*-quinones or other intermediates in melanin biosynthesis, thus delaying oxidative polymerization [93]. Therefore, this notion was confirmed our recent reports in which the melanogenesis inhibitory activity of *A. incisus* extract may be attributed to its anti-oxidative action.

***In vitro* anti–inflammatory activity of *A. incisus* extract**

In order to demonstrate *in vitro* anti-inflammatory effects of *A. incisus* extract, this study was undertaken to investigate its inhibitory effect on the production of TNF-α in RAW 264.7 macrophages activated with the endotoxin LPS. The results showed that *A. incisus* extract showed significant effect on cell viability at the concentration of 60 μg/ml (Table 6) whereas that of prednisolone is at the concentration of 10 μg/ml (Table 7). This destroying may result in decreasing in production of TNF-α. Therefore, the anti-inflammatory activity of *A. incisus* extract was less than that of prednisolone (Appendix D).

Table 6 The inhibitory effect of *A. incisus* extract on TNF-α production and on cell viability of RAW264.7 cells stimulated by 1 μg/mL of LPS (Data are in means±S.D. of triplicate study).

Concentration of *A. incisus* extract (μg/ml)	% TNF-α inhibition	% Cell viability
40	18.3±1.6	99.0±1.7
60	25.0±1.0	96.0±0.8
80	34.2±2.5	95.4±1.1
100	39.8±2.0	93.1±1.4
120	48.7±2.7	89.2±1.3
140	60.7±3.0	88.3±0.6
160	67.4±1.4	85.0±1.0

Table 7 The inhibitory effect of prednisolone on TNF-α production and on cell viability of RAW264.7 cells stimulated by 1 μg/mL of LPS (Data are in means±S.D. of triplicate study).

Concentration of Prednisolone (μg/ml)	% TNF-α inhibition	% Cell viability
5	9.7±1.0	98.7±0.9
10	18.7±2.4	95.1±0.7
15	27.6±2.5	92.1±1.3
20	41.1±3.2	91.6±0.6
25	52.0±2.7	87.9±1.8
30	61.2±3.6	83.9±1.1
35	72.3±1.5	80.2±0.7

It is generally reported that flavonoids have the radical scavenging activity which inhibits NF-κB activation induced by LPS signal resulting in the suppression of TNF-α production [94]. From antioxidant property of *A. incisus* extract as described above, therefore, its inhibitory mode of action on TNF-α production may be medicated by suppressing antioxidation effect. As UVB exposure can lead to systemic immunosuppression possibly via release of soluble mediators such as IL-1α, IL-10, TNF-α and *cis*-urocarnic acid from UVB-irradiated epidermis into the circulation [95]. Therefore, its anti-inflammatory activity would be used to treat of photodamage to reduce redness associated with inflammation.

Physicochemical characterization of nanoemulsions

1. Morphology

The morphology of nanoemulsion was observed by TEM (Figure 30). The droplets in the nanoemulsion appeared dark, and the surroundings were bright. The oil droplets containing *A. incisus* extract were dispersed in the water phase and had an average diameter of about 150-300 nm. This size seemed to be in agreement with the droplet size distribution measured using the Zetasizer.

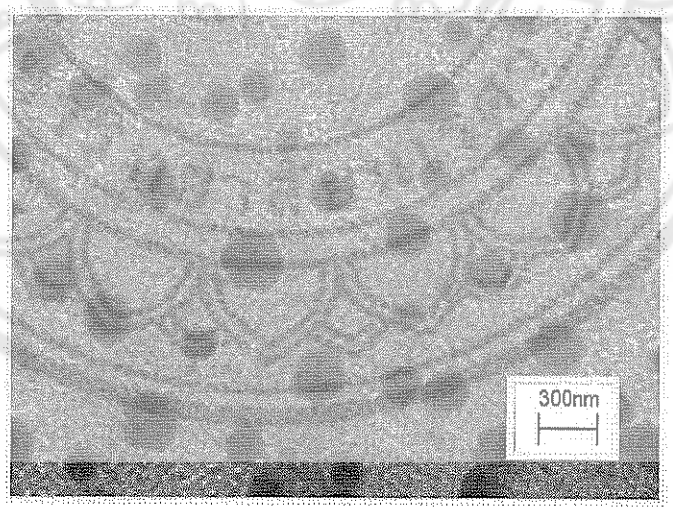

Figure 30 Transmission electron photomicrograph of nanoemulsion formulation consisted of 0.02% w/w *A. incisus* extract, 41.62% w/w isopropyl myristate, 8% w/w ceteareth-10, 5% w/w GMS and 0.03% w/w carbopol 940.

2. Droplet size

The Effects of processing conditions on mean droplet size of nanoemulsions were studied using Photon Correlation Spectroscopy (PCS). The droplet size of the formulation consisted of 8% w/w ceteareth-10 and 5% w/w GMS was the lowest (325±15 nm), which is very well evident from the lowest polydispersity values (0.31±0.02). Polydispersity is the ratio of standard deviation to mean droplet size, so it indicates the uniformity of droplet size within the formulation. The high polydispersity provide the low the uniformity of the droplet in the formulation. All the formulations had droplets in the nano ranges. The mean droplet size of nanoemulsions formulated with different percentages of nonionic emulsifier ceteareth-10 or ceteareth-20, and co-emulsifier glyceryl monostearate (GMS) are shown in Figure 31 to 34 (Appendix E).

The effect of ceteareth-10 on the mean droplet size was observed by varying the surfactant at 4, 8, 10, 12 and 16% w/w while maintaining the amount of GMS at 5% w/w as shown in Figure 28. The results showed that the optimal droplet size of 325±15 nm with polydispersity of 0.31±0.02 was obtained when formulated with 8% w/w of ceteareth-10. When the amount of ceteareth-10 was increased the mean droplet size was also increased. In fact, increasing surfactant should result in smaller droplet size. However the results were unexpected as the larger droplet size was observed as confirmed with PCS. One explanation for the observed aggregation may involve intrinsic thermodynamic instability of the system. As the small particle size possesses high surface area that was energetically in suboptimal state, consequently leading to agglomeration of small particles in order to decrease free energy of system [17].

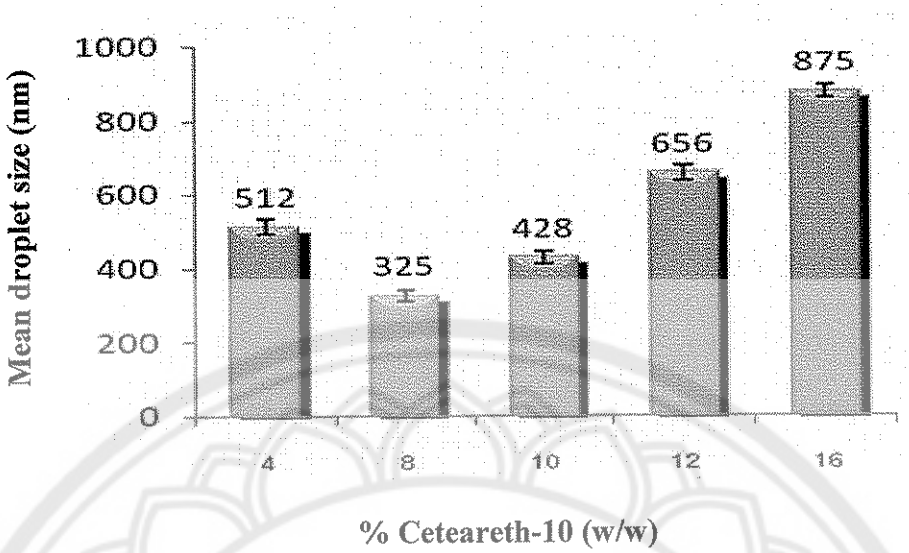

Figure 31 Effect of ceteareth-10 concentration at 4, 8, 10, 12 and 16% w/w while maintaining the amount of GMS at 5% w/w on the droplet size of nanoemulsions (Each bar represents mean±S.D. of triplicate study).

The effect of the amount of GMS mixed with ceteareth-10 on the mean particle size is shown in Figure 32. GMS was varied from 1-8% w/w. The optimum size of 325 nm was obtained when formulated with 5% w/w GMS. The results showed that when increasing concentration from 1-5% w/w, mean particle size was decreased from 409 to 325 nm. In adition, in the case of nanoemulsion without GMS as the coemulsifier, the nanoemulsion showed the mean particle size of 412 nm (data not shown). These results suggested that GMS may stabilize the nanodroplet through steric hindrance of monoester group [96, 97]. When increasing the concentration of GMS to 6% w/w, the mean droplet size and polydispersity value were obviously increased as GMS became predominantly of a solid lipid function when GMS concentration was above 5% w/w. As result, inadequacy of surfactant in the solid lipid system arose and finally led to agglomeration of droplets. Therefore, 5% w/w GMS was found to be an optimum concentration of the formulation.

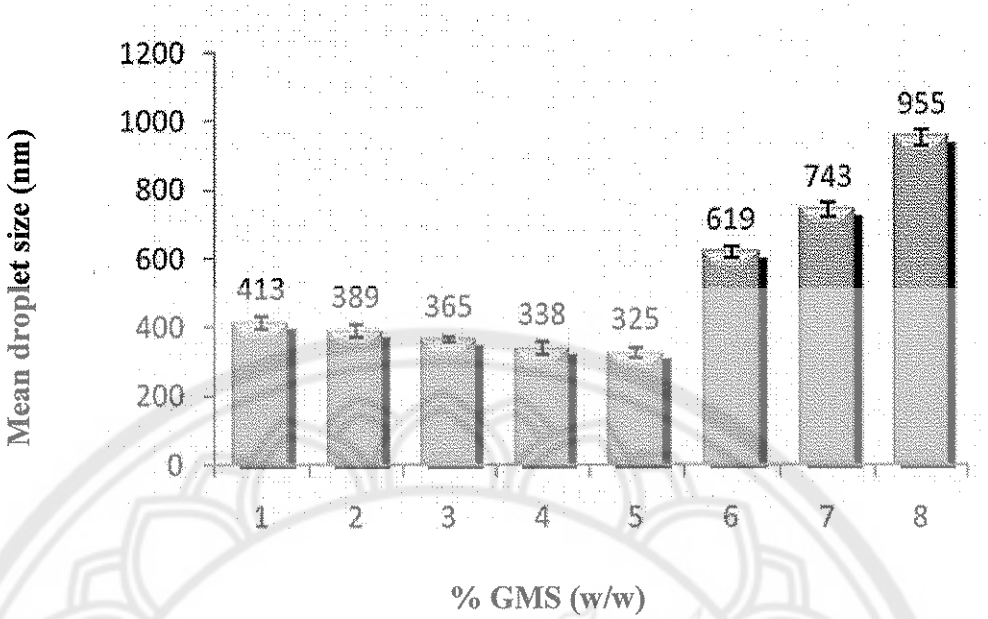

Figure 32 Effect of GMS concentration varied from 1-8% w/w while maintaining the amount of ceteareth-10 at 8% w/w on the droplet size of nanoemulsions (Each bar represents mean±S.D. of triplicate study).

The effect of ceteareth-20 on the mean droplet size was observed by varying the surfactant at 4, 8, 10, 12 and 16% w/w while maintaining the amount of GMS at 5% w/w is shown in Figure 33. The results showed that the all formulations had droplets in nano range. However, the droplet size of formulation containing ceteareth-20 was higher than that of ceteareth-10.

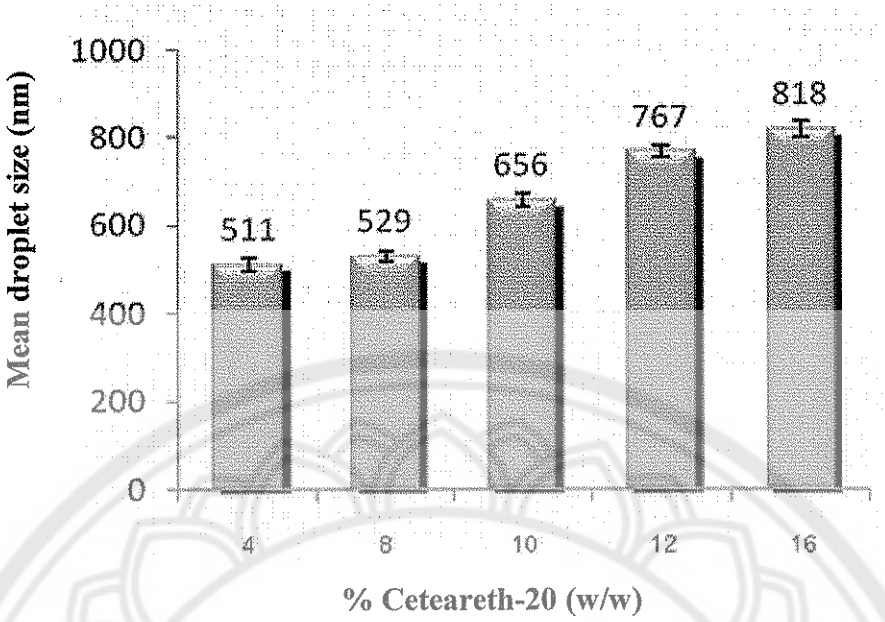

Figure 33 Effect of ceteareth-20 concentration at 4, 8, 10, 12 and 16% w/w while maintaining the amount of GMS at 5% w/w on the droplet size of nanoemulsions (Each bar represents mean±S.D. of triplicate study).

The effect of the amount of GMS mixed with ceteareth-20 on the mean particle size is shown in Figure 34. GMS was varied from 1-8% w/w. The results revealed that as the amount of GMS was increased, the mean particle size decreased. However, increasing GMS concentration more than 4% w/w resulted in larger mean droplet size.

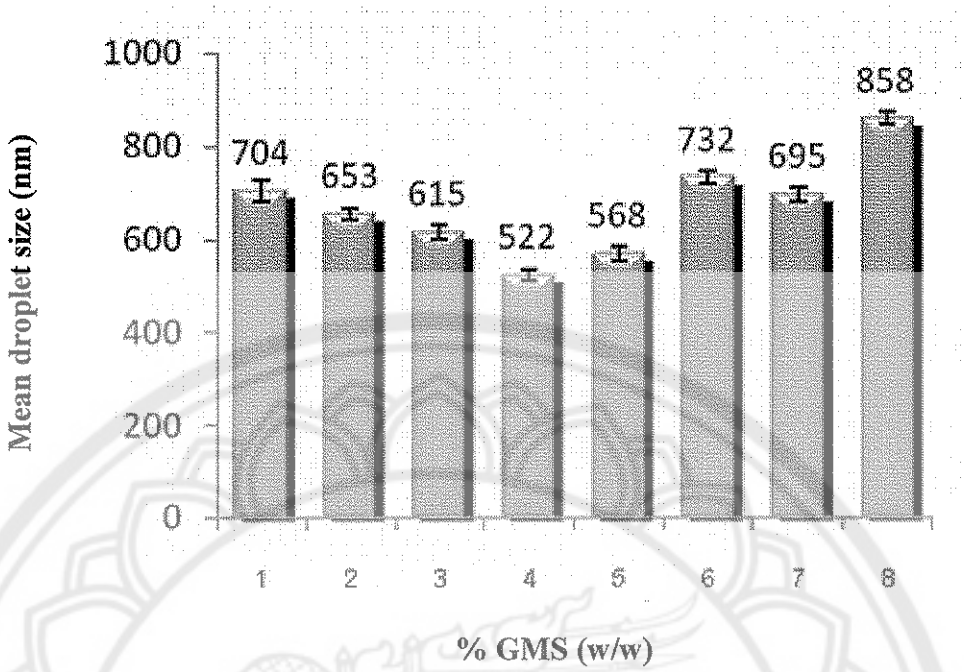

Figure 34 Effect of GMS concentration varied from 1-8% w/w while maintaining the amount of ceteareth-20 at 8% w/w on the droplet size of nanoemulsions (Each bar represents mean±S.D. of triplicate study).

Stability studies of nanoemulsion containing *A. incisus* extract

Nanoemulsion containing *A. incisus* extract was obtained by PIT method. The final products contained 0.02% w/w *A. incisus* extract. The stability of nanoemulsions containing *A. incisus* extract in term of chemical and physical properties was studied.

1. Chemical stability of nanoemulsion containing *A. incisus* extract

The stability of artocarpin in nanoemulsions was studied under both normal condition and stress condition employing 7 heat-cool cycles (4°C for 24 hr and then alternated to 45°C for another 24 hr).

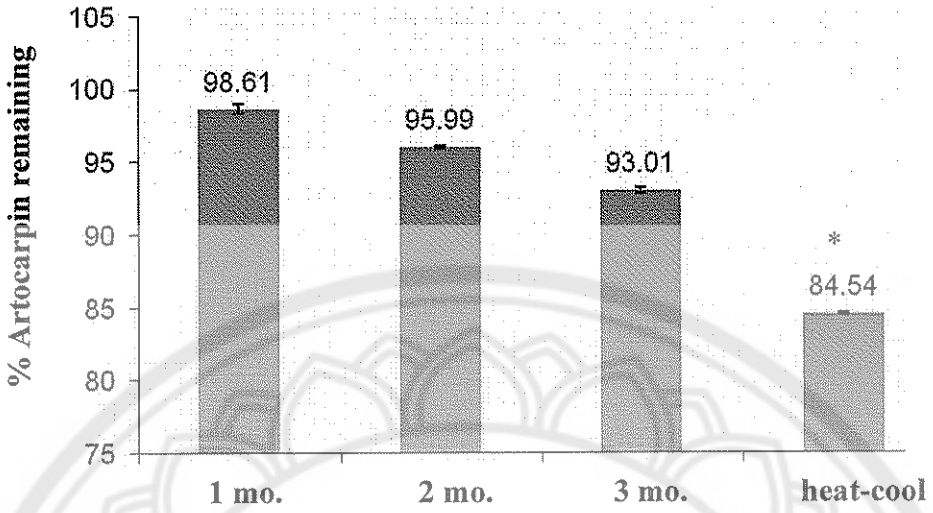

Figure 35 Percentage of artocarpin remaining in nanoemulsion under normal condition for various periods and stress condition employing 7 heat cool cycles (Each bar represents mean±S.D. of triplicate study. Significant differences from freshly prepare; *p<0.05).

As shown in Figures 35, after 7 heat-cool cycles, stress condition and three months storage under normal condition employing room temperature, the percentage of artocarpin remaining after 3 months storage compare to those of freshly preparation was 93.01±0.08% while 84.54±0.32% of artocarpin remaining was obtained under stress condition employing 7 heat-cool cycles (Appendix E).

2. Physical stability of nanoemulsion containing *A. incisus* extract

Physical stability of nanoemulsion containing *A. incisus* extract was studied in terms of droplet size, viscosity and pH value. By using paired t-test, there was no significant different in droplet size, viscosity and pH value after 3 months storage under normal condition at room temperature while the droplet size was less than that after storage under stress condition employing 7 heat-cool cycles, as shown in Figure 36-38 (Appendix E).

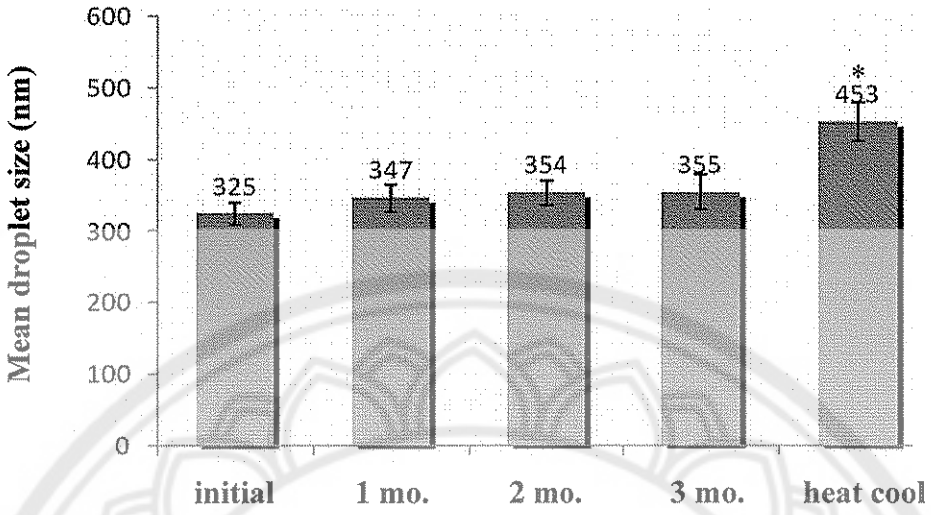

Figure 36 Changes in droplet size of nanoemulsion under normal condition for various periods and stress condition employing 7 heat cool cycles (Each bar represents mean±S.D. of triplicate study. Significant differences from initial; *p<0.05).

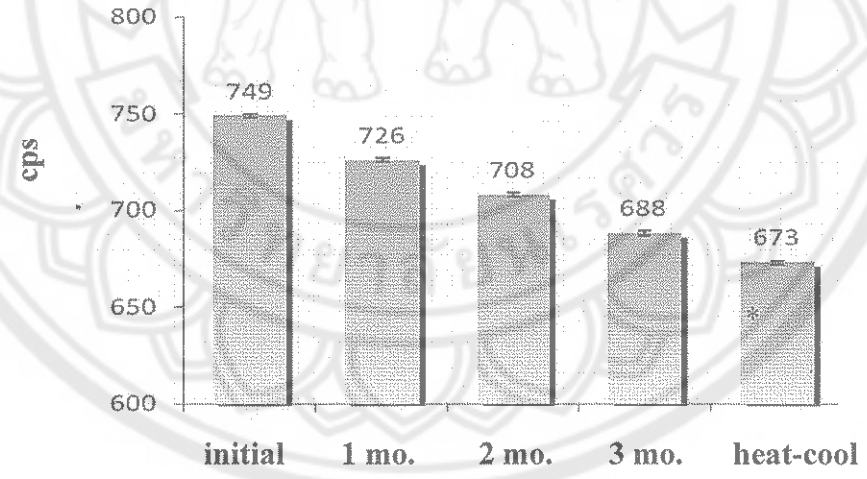

Figure 37 Changes in viscosity of nanoemulsion under normal condition for various periods and stress condition employing 7 heat-cool cycles (Each bar represents mean±S.D. of triplicate study. Significant differences from initial; *p<0.05).

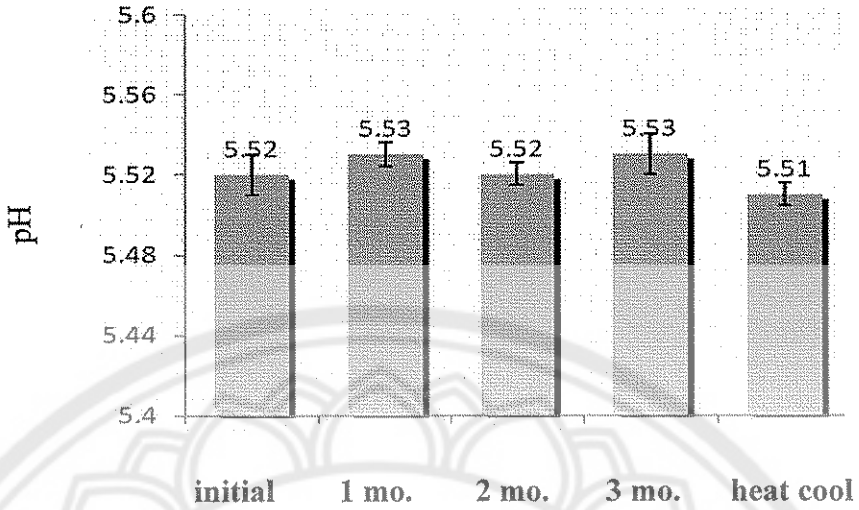

Figure 38 Changes in pH of nanoemulsion under normal condition for various periods and stress condition employing 7 heat cool cycles (Each bar represents mean±S.D. of triplicate study).

However, it has been known for a long time that the finely dispersed oil droplets in PIT emulsions have a strong tendency to coalesce at temperatures near the PIT range [69, 98]. Therefore, one possible way to improve storage stability is adjusted through emulsifier selection far above the usual storage temperatures in a temperature range between 70-90°C [99].

***In vitro* permeation studies through mouse skin**

In vitro skin permeation study was performed to compare the release of artocarpin from nanoemulsion formulation and *A. incisus* extract solution, having the same quantity (0.007 mg) of artocarpin. The percentage of cumulative artocarpins released from nanoemulsion formulation and *A. incisus* extract solution are shown in Figure 39.

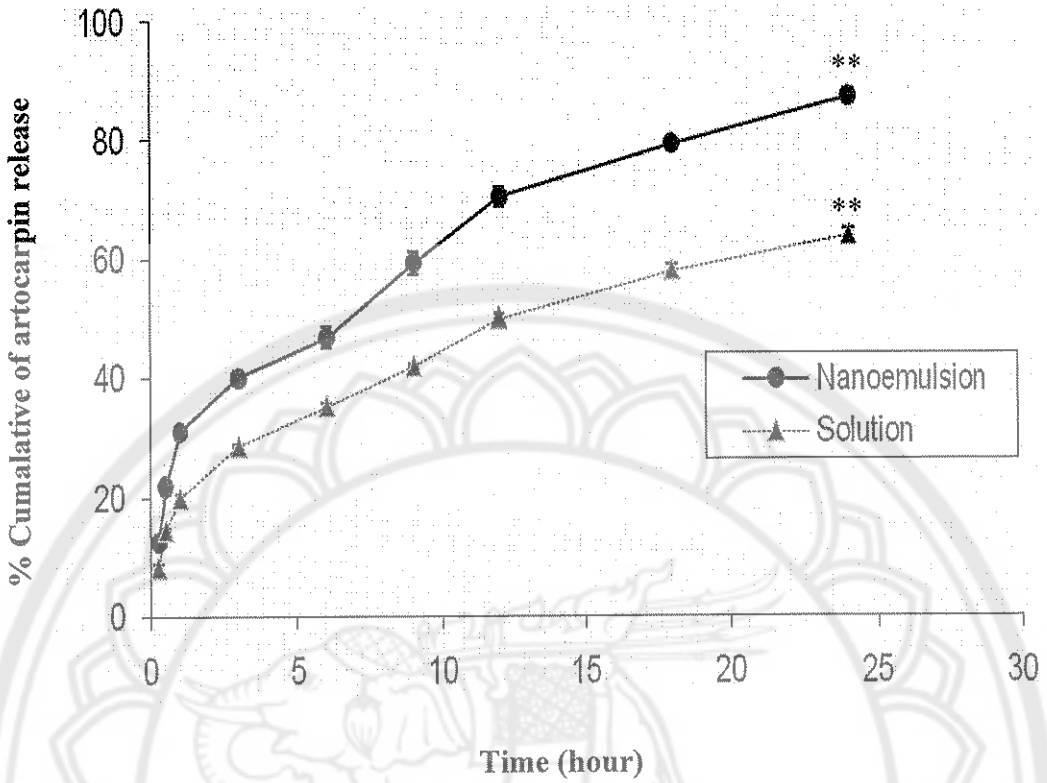

Figure 39 ***In vitro*** **release profile of artocapin from nanoemulsion and** ***A. incisus*** **extract solution (Each point represents mean±S.D. of triplicate study. Significant differences from control; *****p*<0.01).

The percentage of cumulative artocarpin released within 24 hr was 87.2±1.6% from nanoemulsion formulation (Appendix F). The release of artocarpin from nanoemulsion formulation was significantly different when compared with that of *A. incisus* extract solution ($p < 0.01$). The significant difference in artocarpin permeation between nanoemulsion formulation and *A. incisus* extract solution was probably due to the surfactant in nanoemulsion formulation. This is because nanoemulsion component contain permeation enhancers like IPM, ceteareth-10 and GMS.

Additionally, most of the lipophilic drugs pass stratum corneum through an intercellular pathway; a lipid pathway [100]. A dermally applied nanoemulsion is expected to penetrate the stratum corneum and to exist intact in the whole horney layer, alter both lipid and polar pathways [101]. The compound dissolved in the lipid domain of the nanoemulsions can directly penetrate the lipid of the stratum corneum, thereby destabilizing its bilayer structure. These interactions will increase the lipid pathway permeability to compound. When the aqueous fluid of nanoemulsions enters the polar pathway, it increases the interlamellar volume of the stratum corneum lipid bilayer, resulting in disruption of its interfacial structure. A lipophilic compound like artocarpin can then permeate more easily through the lipid pathway of stratum corneum. Moreover, droplet size and viscosity of the nanoemulsion may also affect its efficiency, where the small droplet size and low viscosity of the nanoemulsion make it an excellent carrier for enhancing percutaneous uptake of artocarpin, since the number of vesicles that can interact on a fixed area of stratum corneum will increase when droplet size and viscosity decrease [102]. Therefore, the probably reason for enhanced permeation of artocarpin from nanoemulsion formulation could be the combined effects of hydrophilic and lipophilic domains as well as the small droplet size of nanoemulsion.

***In vivo* studies of UVB-induced hyperpigmentation in C57BL/6 mice**

The whitening effect of nanoemulsion containing *A. incisus* extract was examined under a UVB-induced hyperpigmentation model in C57BL/6 mice. UVB-induced hyperpigmentation was elicited on the dorsal skin of C57BL/6 mice according to a slight modification of the method [81, 82]. Figure 37 shows a photograph of the whitening effect on the C57BL/6 mouse dorsal skin.

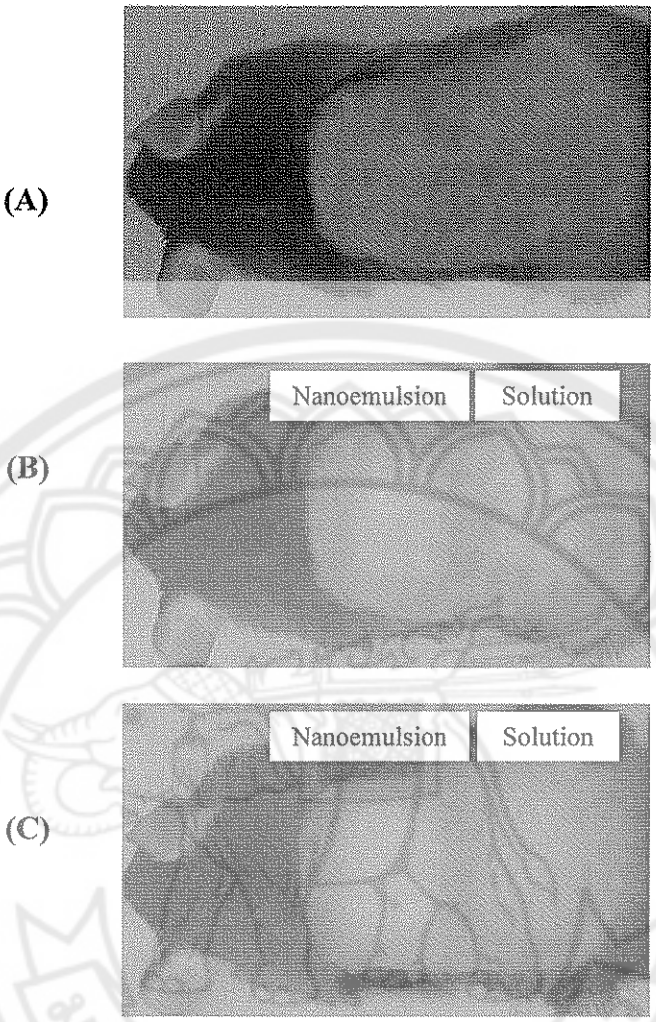

Figure 40 Effect of nanoemulsion containing *A. incisus* extract and *A. incisus* solution on UVB-induced hyperpigmentation in C57BL/6 mouse skin; all photographs are from the same animal (A) initial pigment after UV irradiation and after the topical application, (B) 4 weeks, (C) 6 weeks.

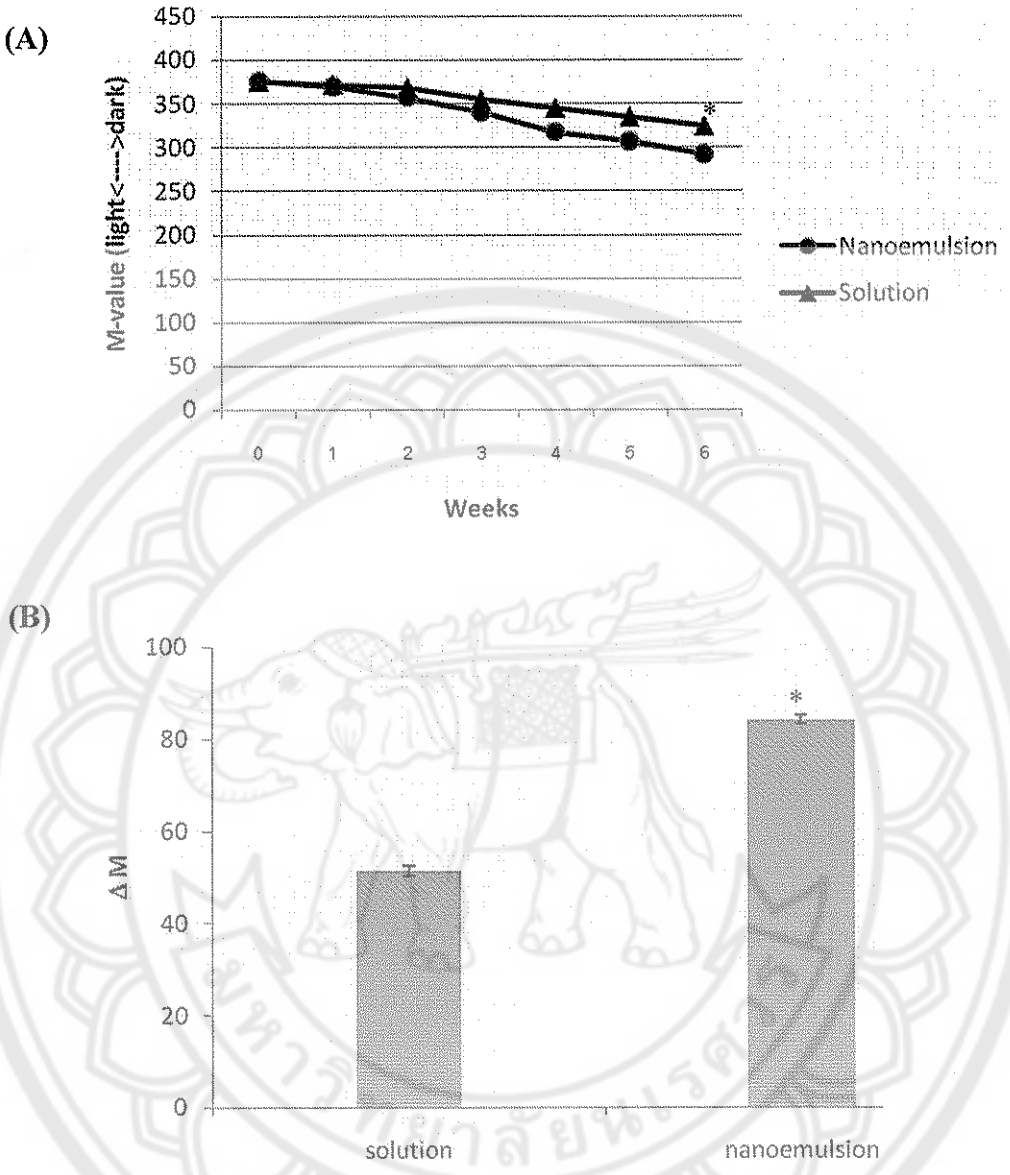

Figure 41 Changes of M-value after the daily topical applications (A) and the degree of pigmentation (ΔM-value) before and 6 weeks after daily topical application (B) of the nanoemulsion containing *A. incisus* extract and *A. incisus* extract solution. (Each point represents mean±S.D. of triplicate study. Significant differences from control; *$p<0.05$).

Nanoemulsion containing *A. incisus* extract was topically applied to the UV-induced hyperpigmented dorsal skin areas twice a day for 6 weeks from the day after the last tanning. As shown in Figure 40B, a visible decrease in hyperpigmentation was observed 4 weeks after the treatment with nanoemulsion containing *A. incisus* extract, when compared to the *A. incisus* extract solution group. Moreover, a strongly visible decrease in hyperpigmentation was observed at 6 weeks after treatment with nanoemulsion containing *A. incisus* extract compared to the *A. incisus* extract solution group as shown in Figure 40C. The degree of pigmentation decreased (ΔM-value) before and 6 weeks after the application of nanoemulsion containing *A. incisus* extract was 84±4 while that of *A. incisus* was 51±3 (Figure 41B, Appendix A). The application of nanoemulsion containing *A. incisus* extract to the skin for 6 weeks caused higher color lightening than *A. incisus* extract solution group ($p < 0.05$). Furthermore, visible edema was not observed at any sites where the dorsal was treated with nanoemulsion containing *A. incisus* extract during all experimental days. Recently, there has been reported that artocarpin showed skin lightening effect on UVB-induced hyperpigmentation dorsal skin of brownish guinea pigs [5]. This probably results from the steric hindrance structure since a 4-substituted resorcinol skeleton, coupled with a C3 substituent presents in the flavone structure of artocarpin [103]. The melanogenesis inhibitory activity of artocarpin may mainly involve in the transportation of tyrosine through the melanosomal membrane which is needed to clarify in the future. Additionally, UV irradiation also increases the generation of ROS in the skin [103] and generated ROS assists melanogenesis [105]. It has been reported that UV irradiation-induced melanogenesis was reduced by the topical application of such antioxidants as vitamin C and E to the skin [106].

Generally, the ideal of whitening agents should have a potent rapid and selective bleaching effect on hyperactivated melanocyte cells and carry no short- or long-term side effect. The result indicated that the lightening effect was observed following the topical application of nanoemulsion containing *A. incisus* extract on UV-stimulated hyperpigmentation. The skin also returned to its original color after stopped treatment. Consequently, with all tests finding taken together, the *A. incisus* extract with antioxidant, melanogenesis inhibitory and anti-inflammatory activities would be used to treat photodamage to reduce skin pigmentation and redness associated with

inflammation. Moreover, nanoemulsions using PIT method are potential vehicles for improved transdermal delivery of the compounds from *A. incisus*'s heartwood extract since the small droplet size can permeate through the skin surface and enhance the skin penetration of active ingredients and thus increase their concentrations in the skin [8].